Evolution of the Strength of Polymer Fiber-Reinforced SCC during Early Hydration

L. K. Mettler; F. K. Wittel; R. J. Flatt; and H. J. Herrmann

Institute for Building Materials, ETH Zurich, Stefano-Franscini-Platz 3, HIF, 8093 Zurich, Switzerland. E-mail: fwittel@ethz.ch

Abstract

Novel fabrication techniques for non-standard concrete structures rely on the interplay of robotic fabrication with the evolution of the material performance, mainly during early hydration. When the material transforms from a yield stress fluid to a cohesive frictional material, detailed knowledge on the evolution of the strength envelope becomes essential. This is even truer, as the dead weight acting on the previously fabricated zones increases with the size of the fabricated structures. A set of non-standard mechanical tests for compression, tension and shear, particularly suited for measuring failure from early hydration states on, exhibits two distinct scaling regimes. The first one is characteristic for large local plastic deformations, followed by the transition to the second regime with material behavior dominated by crack growth. Finally we condense all test results to a limit surface in principal stress space and discuss its evolution with the advancing state of hydration.

INTRODUCTION

The strength evolution during early hydration is of increasing importance for new technologies in concrete fabrication such as robotic slip-forming of concrete pillars with variable cross-sections by flexible actuated formworks. It is significantly smaller than the structures produced and the material leaves the mold during the ongoing early hydration process, while it is still deformable and yet able to provide the strength necessary to sustain its own weight. The trade-off between deformability and strength during hydration restricts the time for active shaping. It is crucial to precisely predict the rheological properties of the material during the early phase of its transition from a complex yield stress fluid to a solid material. We focus on self-compacting concrete (SCC) with and without polymer fibers in an accelerated mixture. Two types of failure constrain the design window: (1) breakdown of the micro-structure due to motion of the formwork caused by the thixotropic nature of SCC, resulting in sudden local liquefaction and following structural collapse and (2) appearance of surface cracks due to forming, caused by the rapid increase in yield stress with respect to the current tensile strength. For such a demanding process, the strength evolution needs to be continuously monitored by means of simple on-line rheological measurements that are related to the known scaling behavior of the failure envelope for the SCC material during early hydration.

To assess the early regime with mechanical tests at diverse stress states, “non-standard” mechanical tests were performed within the described bounds of liquefaction and fracture localization. This work presents results from 4 different test setups on SCC, followed by the discussion of the respective results and their condensation to a set of failure criteria evolving with the advancing state of hydration.

EXPERIMENTAL FINDINGS

The SCC used throughout this study was heavily retarded by means of a sucrose solution (2.7g/l) and subsequently accelerated (60 g/l BASF X-Seed 100). The concrete mixture comprises CEM I 52.5 R Portland cement (981.73g/l Holcim Normo 5R), sand aggregates of up to 4mm in diameter (740.34 g/l), two mineral admixtures fly ash (164.67 g/l Holcim Hydrolent) and silica fume (92.89 g/l Elkem Microsilica Grade 971 U), as well as a superplasticizer (4 g/l BASF Glenium ACE30) as a water reducing admixture and water (371 g/l). Mixtures with and without PVA fiber reinforcement of 6 mm (13 g/l) and 12 mm (13 g/l) were compared. The slump diameter obtained by a Hagermann cone is typically 20- 22 cm and the density of the mixture amounts to 2350 kg/m^3. Special attention was also given to maintaining a uniform mixing procedure for all tests. 5-10 min after completing the mixing with a rotating pan mixer (Zyklos ZK 50 HE), all samples were cast into the respective molds and put to rest. Note that already the short time span of the mold filling makes a noticeable difference in strength evolution due to the thixotropic structural buildup at rest, calling for a correction procedure.

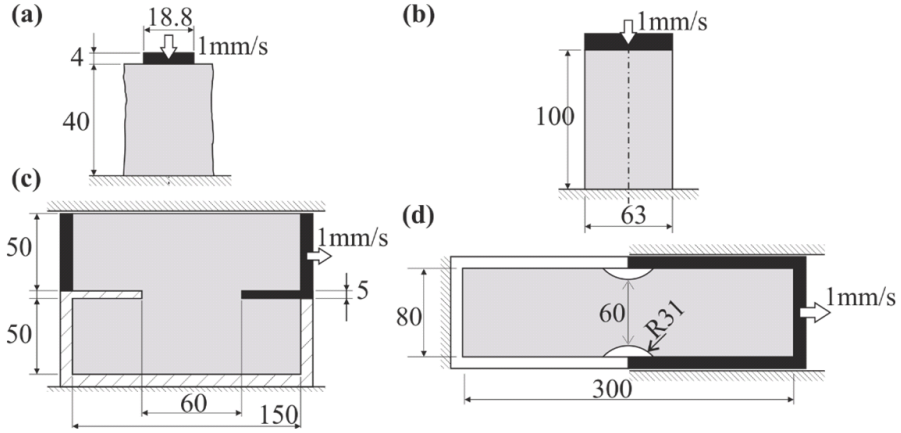

Figure 1: Test setups: (a) penetration of a cylinder into a concrete basin; (b) cylinder compression; (c) shear cell of 60mm depth; and (d) tensile sample of 60mm depth. All dimensions in mm. Moving parts are black, concrete is shaded grey.

Samples were stored and tested at 50%RH/20°C for a period of up to 6 hours after mixing using a triaxial table and a universal testing machine (Zwick 1454). Measurements started as soon as possible with respect to each of the 4 test setups (see Figs. 1a-d), namely: **Test (a) – Penetration** of a rigid cylinder into a basin of concrete similar to ASTM C403/ C403M-08. **Test (b) - Compression** of cylindrical samples, **test (c) - Shear** strength measurements inside molds, in a setup similar to the Jenike shear cell (ASTM D6128-14), as well as **test (d) - Tension** testing inside a mold of two separable parts with a notch. The shear force transmission at the walls of the mold for tests **c** and **d** is assured by several rows of pins along the box walls. Unfortunately, due to the fresh state, an accurate determination of the degree of hydration through calorimetry or other means proved to be unfeasible. A displacement rate of 1mm/s attested to minimize rate effects.

Typical load-displacement curves and identified ultimate load values are shown in Figs. 2 a-d for polymer fiber reinforced concrete (FRC). By normalization with the

respective reference areas of the tests, time dependent strength values are obtained. However to correct for differences in the onset of the evolution e.g. due to different molding times or between different series, each set is corrected to obtain the data collapse shown in Figs. 2A,B. For comparison, the curves for plain SCC without fibers are added. Corrections are based on the observation that penetration data (test a) from within one mixture follows approximately an exponential evolution law $S=a\cdot exp(bt)$ between 0.01-1MPa with similar exponents in between sets. Hence all data form a master curve that can be used for mapping the evolution. Also gravitational loads are added to the measured force.

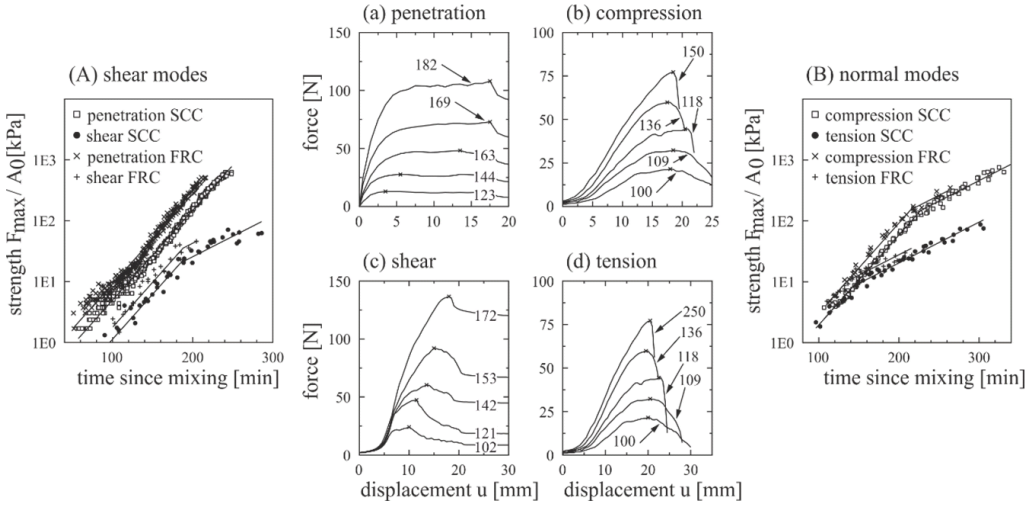

Figure 2: Exemplary force-displacement curves (a-d) and corrected time dependent strength evolution for shear mode (A) and normal mode (B) failure.

Two principal regimes seem to govern the strength evolution: A first one, where material is deformed in a ductile way and shear, compressive and tensile strengths are well-represented by the Mises criterion. An identical exponent of b=0.033min^{-1} and pre-factor a=0.07kPa describes this regime. In the second regime cracks begin to prevail (see Fig. 3b), and failure is increasingly dependent on the hydrostatic component of stress, as seen e.g. by the divergence between compressive and tensile strengths. The exponents b are around 0.014min^{-1}, but the main differences between tensile and compressive strength originates from differences in transition time between the two regimes.

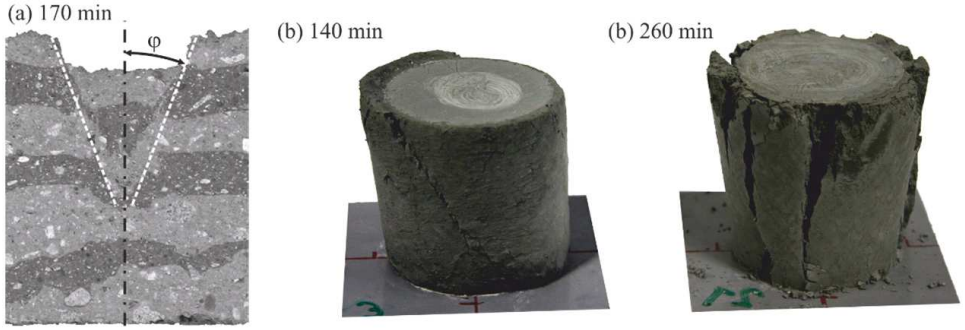

Figure 3: Compression cone test (a), crack patterns test (b) at different times.

CONCLUSIONS

Our study captures the strength evolution of the initially ductile material to a point where failure is brittle and starts to become dependent on hydrostatic stress. We find two scaling regimes of strength that are also evident in the constructed failure envelopes in the principal stress space in Fig. 4. The isochronous limit curves follow thermodynamic principles and material symmetry. At early times a von Mises type behavior fits the experimental data best, while at later times a pressure sensitive behavior emerges due to the different times of regime change of each test setup. The effect of the fibers is shown by comparing FRC to SCC. As expected FRC values are higher throughout the evolution. Note that strength values for shear are corrected by a factor of 1.4 to account for strength increase due to the unsuitability of the shear cell when cohesive properties become increasingly important.

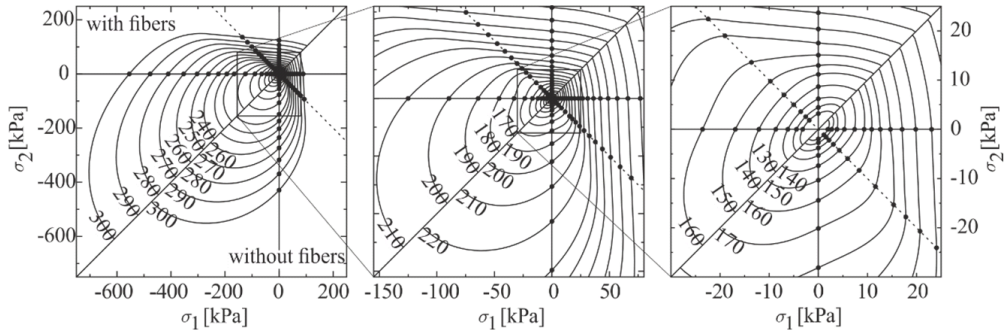

Figure 4: Fitted isochronous failure envelopes with time in minutes from mixing. The upper left envelopes represent FRC, while the lower right ones are fitted to data obtained on SCC without fiber reinforcement.

The time frame of this study was chosen to be up to 6 hours after mixing, keeping the technological design window of the adaptive slip casting process in mind. For such processes it is crucial to precisely predict the rheological and mechanical properties of the material during the early phase of its transition from a non-Newtonian yield stress fluid to a cohesive frictional material.

ACKNOWLEDGEMENT

We acknowledge the support by the ETH Zurich under ETHIIRA grant no. ETH-13 12-1 “Smart Dynamic Casting”.

REFERENCES

[1] Bullard, J. W., Jennings, H. M., Livingston, R. A., Nornat, A., Scherer, G. W., Schweitzer, J. S., Scrivener, K. L., and Thomas, J. J. (2011). “Mechanisms of cement hydration.” *Cem. Concr. Res*. 41, 1208-1223.

[2] Lloret, E., Shahab, A. R., Mettler, L. K., Flatt, R. J., Gramazio, F., Kohler, M., and Langenberg, S. (2014). “Complex concrete structures merging existing casting techniques with digital fabrication.” *Comput. Aided Design* 60, 40–49.

[3] Lootens, D., Jousset, P., Martinie, L., Roussel, N., and Flatt, R. J. (2009). "Yield stress during setting of cement pastes from penetration tests." *Cem. Concr. Res.* 39, 401-408.
[4] van Mier, J. G. M. (1997). *Fracture Processes of Concrete*. CRC Press.